Validation of the Experimental Whole-body SAR Assessment Method in a Complex Indoor Environment

Aliou Bamba*, Wout Joseph, Günter Vermeeren, Emmeric Tanghe, and Luc Martens
Department of Information Technology, Ghent University / IBBT, Ghent, Belgium
*Corresponding author e-mail: aliou.bamba@intec.ugent.be

ABSTRACT

An experimental method accounting the Line-Of-sight (LOS) component and the diffuse multipath components (DMC) to assess the whole-body specific absorption rate (SAR_{wb}) in a complex indoor environment was previously proposed; we validate it now by numerical simulations with the Finite-Difference Time-Domain (FDTD) method. Results show good agreement between measurements and computation at 2.8 GHz for the considered scenarios.

INTRODUCTION

The International Commission on Non-Ionizing Radiation Protection (ICNIRP) defines the SAR as a basic restriction for human exposure in the radio frequency (RF) band. Various works have assessed the whole-body specific absorption rate in indoor environments. In [1], the SAR_{wb} is calculated from measurements data obtained with Personal Exposure Meters, [2] simulates a room with thin plates of materials having different properties, [3] has adequately predicted the RF-electromagnetic fields exposure for outdoor scenarios, but the indoor scenarios were not as successful because of the considerable simplifications made for the investigated indoor environment. The objective of this paper is the validation of the experimental assessment method [4, 5] of the SAR_{wb}. The SAR_{wb} dependency to the DMC is also evaluated and discussed for two scenarios. The FDTD numerical calculations are performed under the same propagation and phantom conditions as in the experimental approach.

MATERIALS AND METHODS

Five identical cylindrical phantoms in polyvinyl chloride (PVC) with an inner radius of 119.5 mm, an outer radius of 124.5 mm (thickness = 5 mm), and a height of 1500 mm have been used (filled with water, σ= 1.58 Ω^{-1}/m (conductivity), ε_r= 77.32 (relative permittivity) and ρ= 1000 kg/m^3 (mass density)) to assess the absorption cross section (ACS) of one phantom like in [4]. Figure 1 shows the location of the phantoms (for the assessment of the ACS) in the investigated room.

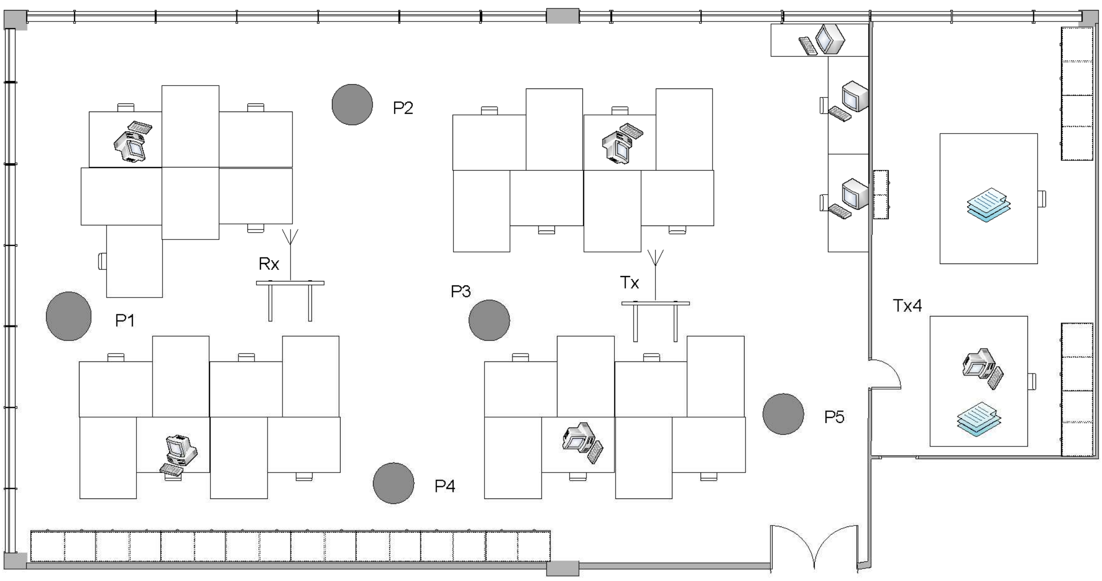

Figure 1: Phantoms location in the room

The SAR_{wb} is calculated for the following scenarios: in scenario A, the phantom is located first at the reverberation distance, i.e., the LOS component and the DMC power densities are the same, (about 6 m in the investigated room, the room volume is about 360 m^3) and in scenario B the phantom is located at 10 m from the transmitter (where the DMC power density is dominating). These scenarios were considered to satisfy the far-field assumption. The transmitter is located at 1.80 m above the ground.

The experimental LOS component power density is determined by the Friis equation and the DMC power density addressed in [6] expression is:

$$I_{dif} = \frac{P_0}{\pi \eta A} e^{-\frac{d_0}{c\tau}} . \eta_{pol} \tag{1}$$

where P_0, η, A, d_0, *c*, τ and η_{pol} are the transmitted power, the fraction of energy absorbed by the surfaces, the total area of the room, the distance Tx-phantom, the light velocity, the reverberation time of the room and the polarization factor in diffuse fields, respectively. The polarization factor is set to 0.5 assuming a complete diffuse field. The experimental SAR_{wb} is expressed as:

$$SAR_{wb}^{\exp} = SAR_{wb}^{\exp,los} + SAR_{wb}^{\exp,dif} = \frac{ACS_{cyl}^{los} \times I_{los}}{m} + \frac{ACS_{cyl}^{dif} \times I_{dif}}{m} = \frac{ACS}{m}\left(I_{dif} + \frac{1}{\pi} I_{los} \right) \tag{2}$$

where $SAR_{wb}^{\exp,los}$, $SAR_{wb}^{\exp,dif}$, m, I_{dif}, I_{los}, and ACS ψrepresent the whole-body specific absorption rate due to the LOS component, the whole-body SAR due to the DMC, the mass of the phantom, the total power density of the DMC, the power density of the LOS component, and the ACS of the phantom, respectively.

For the numerical simulations, we used the SEMCAD-X (Schmid & Partner Engineering AG, www.semcad.com) simulation platform. The maximum grid step in the cylindrical phantom equals $0.07\lambda_{\psi\psi}$, where $\lambda_{\psi\psi}$ $\psi$is the wavelength in the phantom. To avoid reflections of the waves impinging on the boundaries into the simulation domain, uniaxial perfectly match layer (UPML) is used as absorbing boundary conditions. The UPML has been set so that more than 95% of the power of incident waves will be absorbed by the boundary layers. The DMC is modeled with 81 plane waves surrounding the phantom as follows: the DMC are assumed to have a white azimuthal spectrum and uniformly distributed arrival delays in time; the elevation is assumed to be in the horizontal plane. The amplitudes of the plane waves used to model the DMC follow an exponential decay with a damping factor being the reverberation time of the empty room. The directions of arrival of the LOS component are determined by means of the Space-Alternating Generalized Expectation-Maximization Algorithm (SAGE).

RESULTS

We obtained from measurements an average value of the ACS of the phantom of about 0.39 m^2. The total power density for scenarios A and B are 4.30 mW/m^2 and 2.00 mW/m^2, respectively. The experimental $SAR_{wb}^{\exp}$ for the scenario A is 16.10 μW/kg (the SAR induced by the DMC represents 75% of the total absorption rate) whereas the total absorption rate for the scenario B is about 9.90 μW/kg (the SAR induced by the DMC represents 92%).

Table I shows the results of the numerical simulation and the relative deviation with respect to the experimental results. The specific absorption rate induced by *only* the DMC is also listed ($SAR_{wb}^{fdtd,dmc}$).

	DMC(no. of plane waves)	81
Scenario A	SAR_{wb}^{fdtd} (μW/kg)	15.48 μW/kg
	$SAR_{wb}^{fdtd,dmc}$ (μW/kg)	11.47 μW/kg
	Part of DMC in the SAR_{wb}^{fdtd}	74.09 %
	Relative deviation (ΔSAR)	4.00 %
Scenario B	SAR_{wb}^{fdtd}	9.83 μW/kg
	$SAR_{wb}^{fdtd,dmc}$	8.74 μW/kg
	Part of DMC in the SAR_{wb}^{fdtd}	88.91 %
	Relative deviation (ΔSAR)	0.71 %

Table I: Whole-body SAR from simulations

Simulating the DMC with more plane waves was not possible, probably due to software and/or hardware limitations; however 81 plane waves are sufficient to obtain the desired accuracy.

As expected, the high power density in scenario A results in a higher absorption rate. The simulation evidences a relative deviation from the experimental approach of 4 % and 0.71 % for scenarios A and B, respectively, showing that both methods agree excellently. Moreover, the DMC contribution calculated from the simulation is of the same order with the one derived in the experimental approach.

CONCLUSIONS

A method to assess experimentally the whole-body average specific absorption rate in a complex indoor environment is validated through numerical simulations. Two scenarios are investigated to ensure the validity of the method at different locations within the investigated room. Experimental and numerical results agree very well. From both measurements and simulations it turns out that the contribution of the DMC in the induced whole-body specific absorption rate cannot be neglected.

ACKNOWLEDGMENT

The research leading to these results has received funding from the European Union’s Seventh Framework Programme ([FP7/2007-2013]) under grant agreement no 244149. Wout Joseph is a Post-Doctoral Fellow of the FWO-V (Research Foundation - Flanders).

REFERENCES

[1] Wout Joseph, Gunter Vermeeren, Leen Verloock, and Luc Martens. Estimation of Whole-Body SAR From Electromagnetic fields Using Personal Exposure Meters. Bioelectromagnetics 31: 286-295, 2010.

[2] Bernardi P, Cavagnaro M, Cicchetti R, Pisa S, Piuzzi E, Testa O. A UTD/FDTD Investigation on Procedures to Assess Compliance of Cellular Base-Station Antennas With Human-Exposure Limits in a Realistic Urban Environment. IEEE Transactions on Microwave Theory and Techniques 51: 2409-2417, 2003.

[3] Bürgi A, Frei P, Theis G, Mohler E, Braun-Fahrländer C, Fröhlich J, Neubauer G, Egger M, Röösli M. A model for Radiofrequency Electromagnetic Field Predictions at Outdoor and Indoor Locations in the Context of Epidemiological Research. Bioelectromagnetics 31: 226-236, 2010.

[4] A. Bamba, J. B. Andersen, W. Joseph, D. Plets, E. Tanghe, G. Vermeeren, J. O. Nielsen and L. Martens. Experimental Specific Energy Absorption Rate Assessment from Absorption Cross Section Measurement for Far-field Exposure at 2-3 GHz”, in 33rd Annual Meeting of the Bioelectromagnetics Society, Halifax, CA, June 2011. (Accepted)

[5] A. Bamba, W. Joseph, J. B. Andersen, E. Tanghe, G. Vermeeren, D. Plets, J. O. Nielsen and L. Martens. Experimental Assessment of Specific Absorption Rate Using Room Electromagnetics" IEEE Transactions on Electromagnetic Compatibility, 2011. (Accepted with minor revisions).
[6] Andersen J.B, Chee KL, Jacob M, Pedersen GF, Kürner T. Reverberation and Absorption in an Aircraft Cabin with the Impact of Passengers. IEEE Antennas and Propagation Transactions (accepted for publication), 2011.